Supporting Information

Grafting and Controlled Release of Antimicrobial Peptides from Multifunctional Mesoporous Silica

Mohadeseh Bagherabadi[a], Marie Fleckenstein[a], Oleksandr Moskalyk[a], Andrea Belluati[a], Olga Avrutina[a], and Annette Andrieu-Brunsen [a]*

a. Department of Chemistry, Technical University of Darmstadt, Peter-Grünberg-Str. 8, 64287 Darmstadt, Germany.

* annette.andrieu-brunsen@tu-darmstadt.de

Table of Contents

Characterization

Characterization of C14R and Melittin with HR-ESI-MS

To confirm success of solid-phase peptide synthesis, HR-ESI-MS measurements of C14R antimicrobial peptide (Figure S1, top panela) and Melittin (Figure S1, bottom panel) were conducted (Table S1). Figure S1-a shows the m/z patterns corresponding to $[M+2H]^{2+}$, $[M+3H]^{3+}$, and $[M+4H]^{4+}$ species of C14R peptide, respectively melittin. Based on the mass-to-charge ratio of all species for the two peptides, the exact molecular weights of C14R and Melittin were determined to be 2005.40 and 2846.46 Da, respectively, confirming that the synthesis was successful.

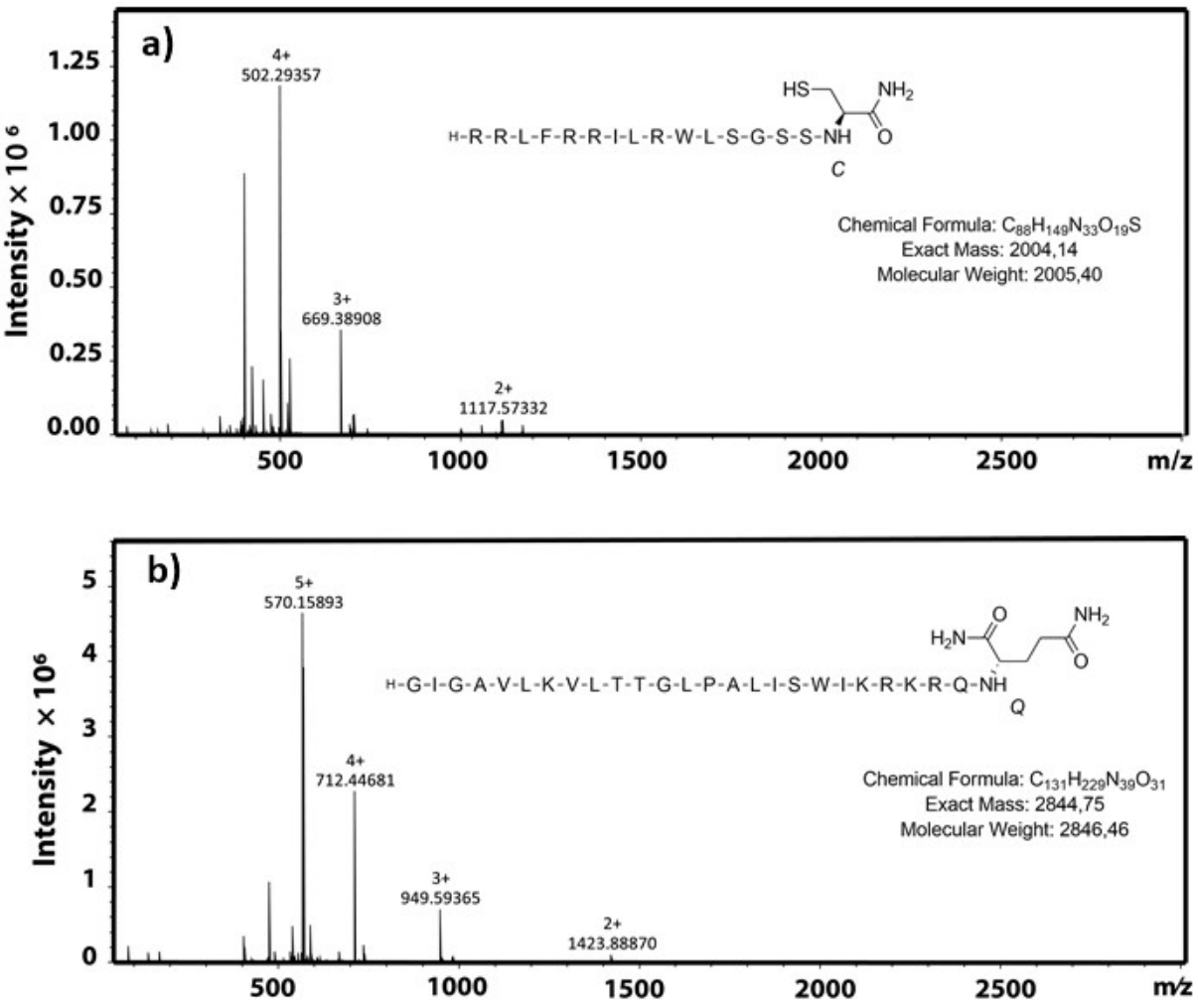

Figure S1. Mass spectrometry (HR-ESI-MS) data for C14R and melittin antimicrobial peptides. (a, b) C14R, (c, d) melittin.

Table S1. HR-ESI_MS from the synthesized peptides, simulated and measured m/z value and the retention times (Rt).

Peptide	Calculated molecular mass (g/mol)	HR-ESI-MS: simulated m/z pattern	HR-ESI-MS: Measured m/z pattern	Rt (min)
C14R	2005.40	502.29365 669.38911 1003.58003	502.29357 $[M+4H]^{4+}$ 669.38908 $[M+3H]^{3+}$ 1117.57332 $[M+2H]^{2+}$+2TFA	11.5
Melittin	2844.46	570.15868 712.44653 949.59295 1423.88579	570.15893 $[M+5H]5^{+}$ 712.44681 $[M+4H]^{4+}$ 949.59365 $[M+3H]^{3+}$ 1423.88870 $[M+2H]^{2+}$	12.0* 12.6*

*The peptide melittin was eluted in two fractions, both exhibiting the same m/z pattern upon ESI-MS analysis.

High-Performance Liquid Chromatography-Mass Spectrometry (HPLC-MS) Analysis

LC-MS of the peptides synthesized were performed using a Shimadzu LC-MS 2020 instrument and a Phenomenex Jupiter C4 (50×1 mm, 5 µm, 300 Å) column with linear acetonitrile gradients in water and a flow rate of 0.2 $mL.min^{-1}$ (see Figures S2). The HPLC analysis of the synthesized C14R and melittin antimicrobial peptides revealed sharp and well-defined peaks, indicating successful synthesis and purification (Figure S2).

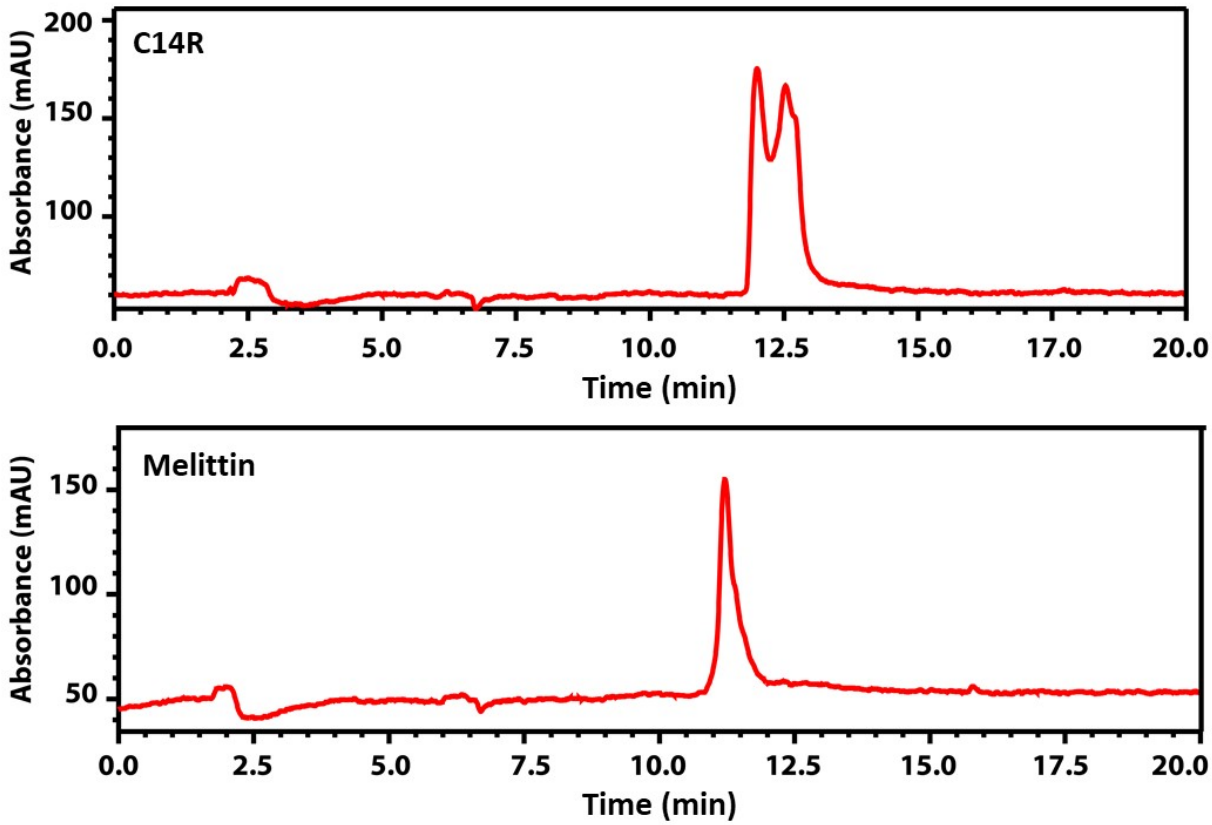

Figure S2. HPLC analysis of synthesized C14R and melittin antimicrobial peptide.

High-Performance Liquid Chromatography (HPLC) was employed to analyze the impact of light irradiation on the C14R antimicrobial peptide. The blue light with a wavelength of 460 nm (11.1 $mWcm^{-2}$) and green light (8.3 $mWcm^{-2}$) with a wavelength of 510-580 nm (Figure S3) were applied for 1 hour. Irradiation did not cause any structural damage to the peptide as deduced from the HPLC profile after irradiating the peptide solution with both green and blue light. This observation implies that there was no discernible effect on the peptide's integrity, confirming the stability of the peptide under release conditions (Figure S4).

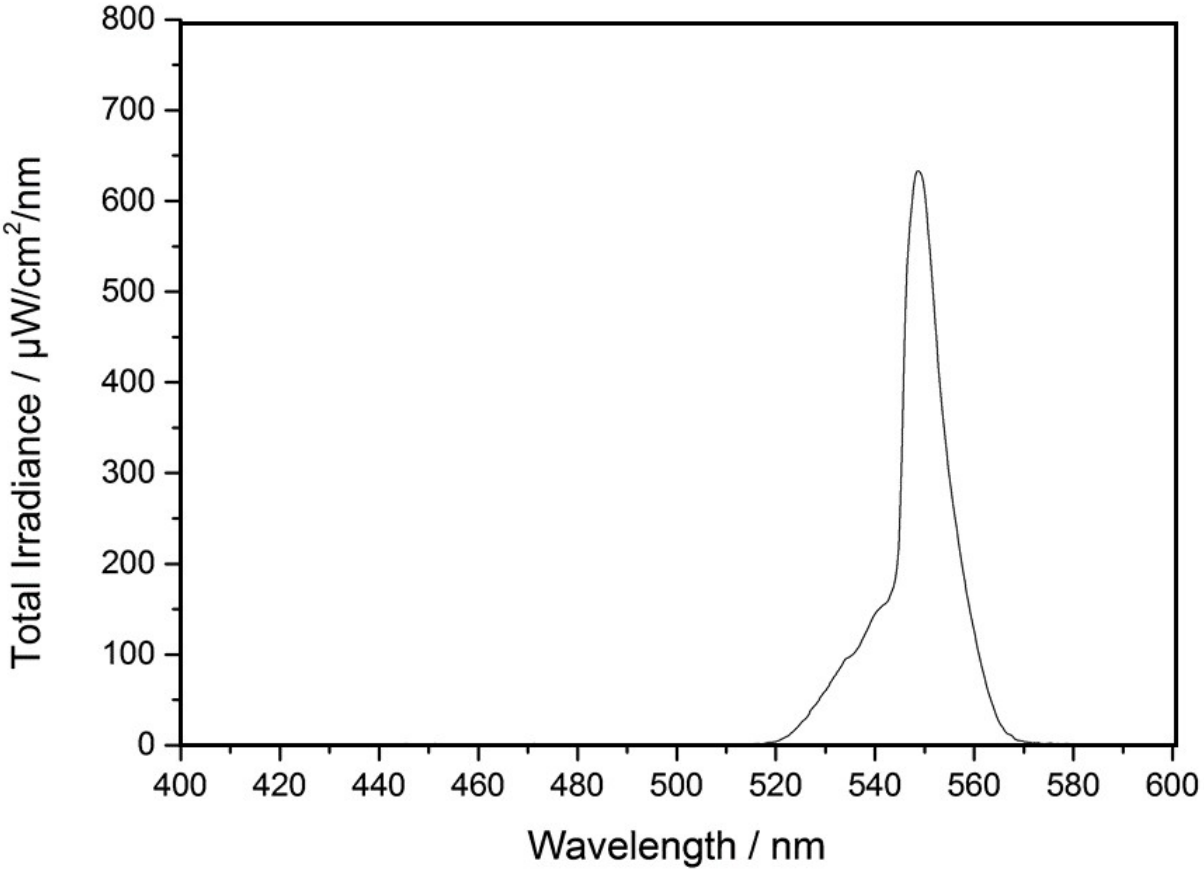

Figure S3. Graph showing the relationship between total irradiance and wavelength for the light source (Superlite, Lumatec, Germany) utilized in photo-release experiments.

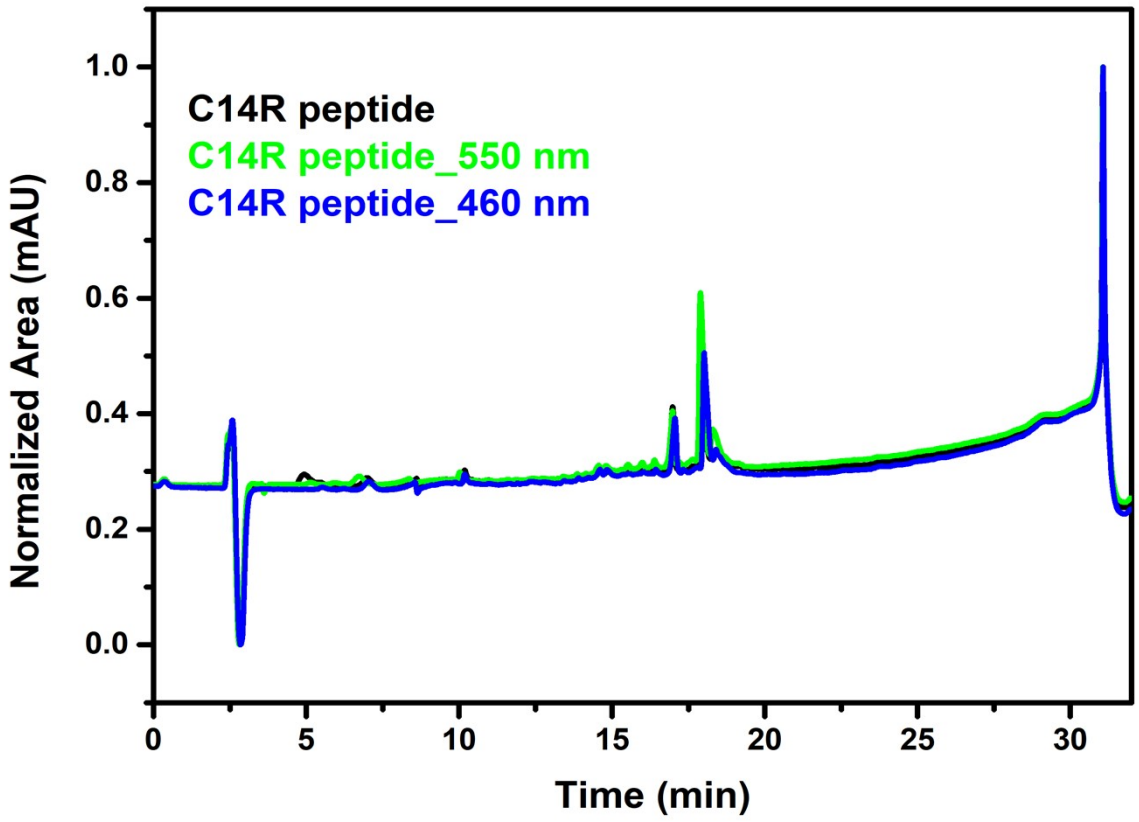

Figure S4. HPLC of C14R antimicrobial peptide without irradiation (black), 1 h irradiation with 550 nm wavelength (green), 1 h irradiation with 480 nm wavelength (blue). Solvent: 1×PBS pH 7.4.

Ellipsometry measurements

In Table S2, the ellipsometry measurements from the replication experiment from mesoporous silica film are listed.

Table S2. Ellipsometry results from mesoporous silica film to determine porosity.

Layer	Position	n	∆n ±	d_{nm}	Δd_{nm} ±	RMSE
SiOx-layer	1			2.3	0.1	0.197
SiO_2-mesoporous	1	1.073	0.029	526.5	40.3	9.09
	2	1.071	0.011	667.1	29.8	8.93
	3	1.121	0.011	650	16.6	7.13

SEM analysis of mesoporous silica film

The top view and cross-sectional images of the mesoporous silica film are shown in Figure S5a-c. SEM images confirm a film thickness in the range of the value detected by ellipsometry, and a homogeneous film thickness.

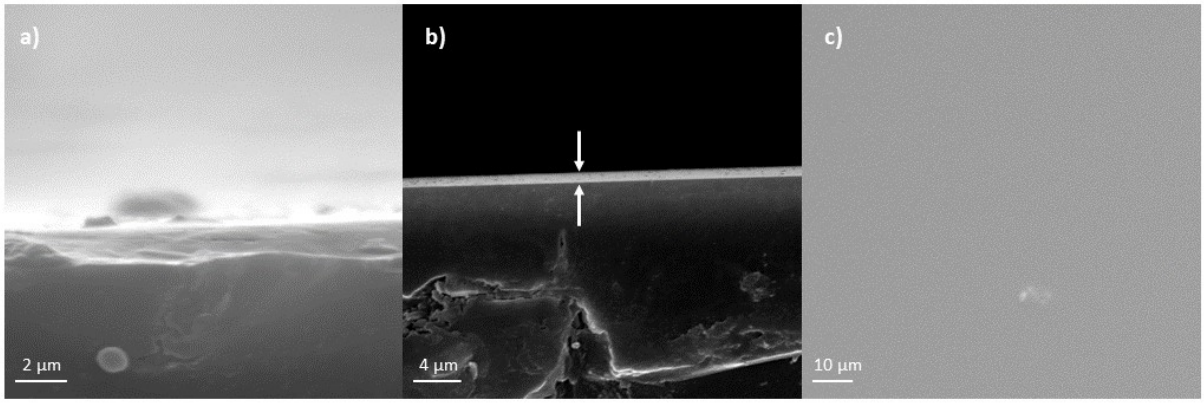

Figure S5. (a, b) Cross-section SEM image from mesoporous silica film, and (c) Top view SEM image of the mesoporous silica film.

Fluorescence and UV-Vis Spectra

To analyze the fluorescence intensity of the mesoporous silica particles that had been functionalized with BODIPY, and C14R grafting dissolved in DMSO as a solvent. The solutions underwent fluorescence spectroscopy detecting the emission wavelengths range from 500 to 650 nm upon excitation at 480 nm with a resolution of 1 nm (as shown in Figure S6). Only a small shift of the fluorescence spectra to longer wavelength of the BODIPY functionalized mesoporous silica particles as compared to particles functionalized with both BODIPY and C14R was observed. This finding suggests that the irradiation light can be relied upon for data, considering the consistent changes in intensity observed in the fluorescence images. Additionally, confirmation of these findings was obtained through UV-vis spectra analysis of the samples (Figure S7).

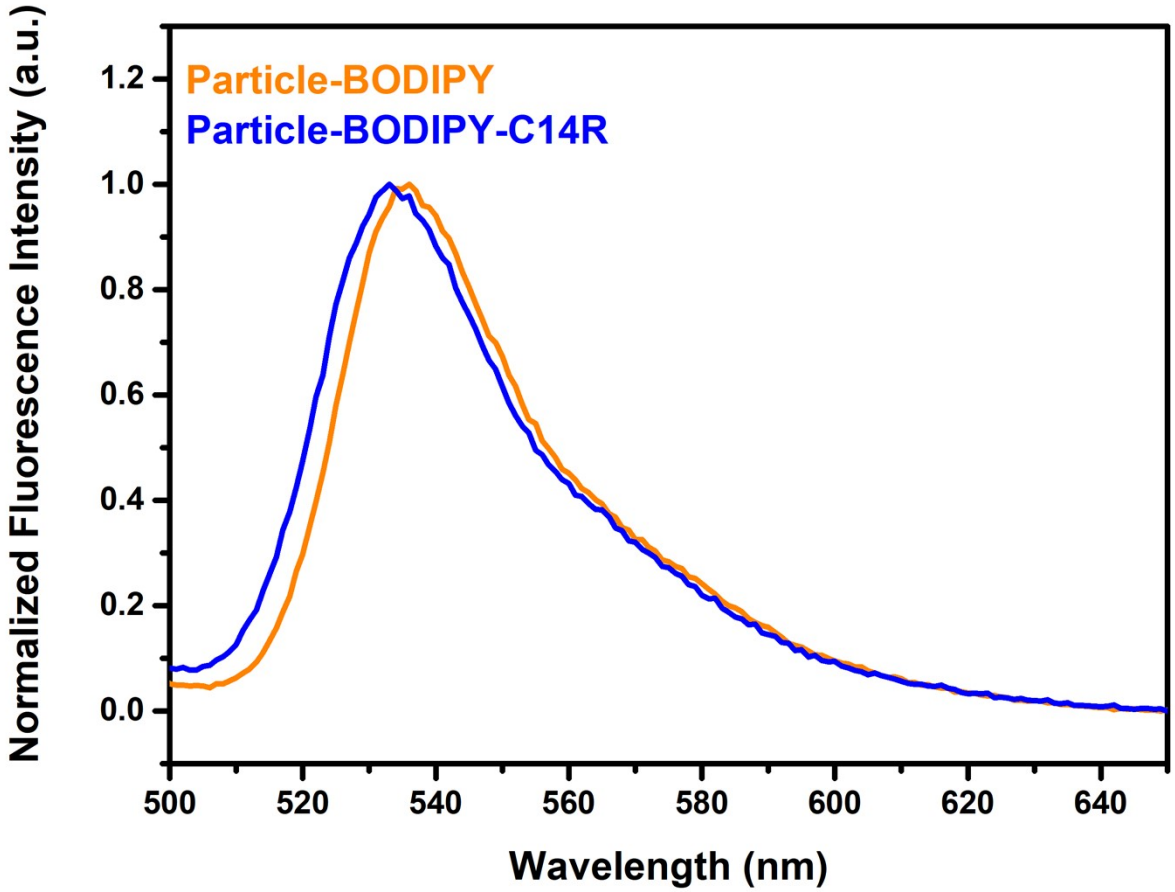

Figure S6. Fluorescence spectra of mesoporous silica particles with PPTESO-BODIPY (orange line), and PPTEOS-BODIPY-C14R (blue line) functionalization. These spectra were obtained by exciting samples at 480 nm and emission was recorded from 500 to 650 nm.

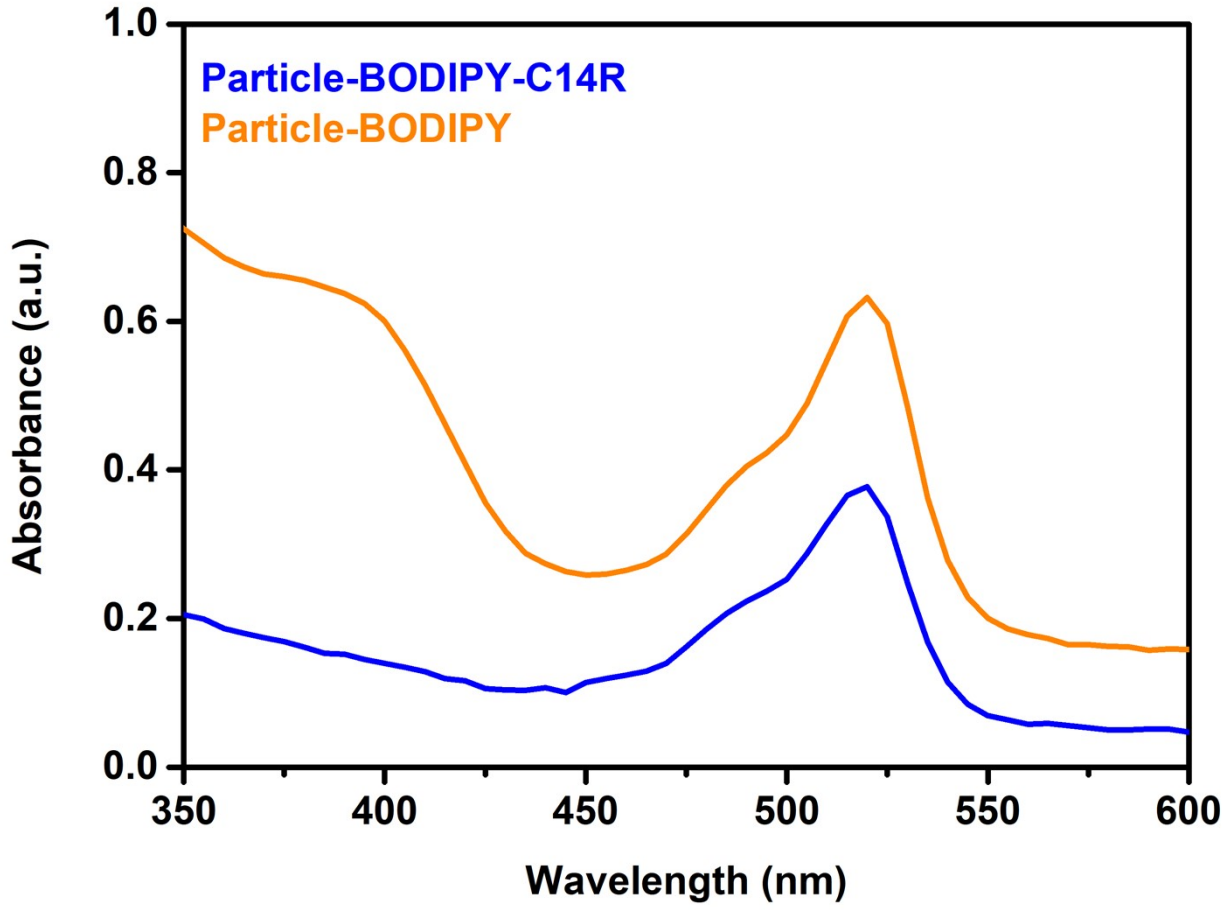

Figure S7. UV-VIs spectra of samples with PPTESO-BODIPY (orange line), and PPTEOS-BODIPY-C14R (blue line) conjugation to the particles.

ATR-IR from C14R Peptide-Mesoporous Silica Particle with Water as a Reference

To demonstrate that the peptide is stably included into the particle, the mesoporous silica particles were immersed in water for 40 minutes, followed by centrifugation of the solution. Subsequently, the particles were dried at ambient atmosphere, and an ATR-IR spectra was recorded (Figure S8, green). The vibrational band at 1658 cm^{-1} related to C=O (amide I) revealed that the present of the peptide in the particle. The vibrational band at 1658 cm^{-1} does not show changes for both samples before and after extraction. The band remains consistently in contact with water, indicating that the peptide remains stable within the silica under the experimental conditions applied. (Figure S8).

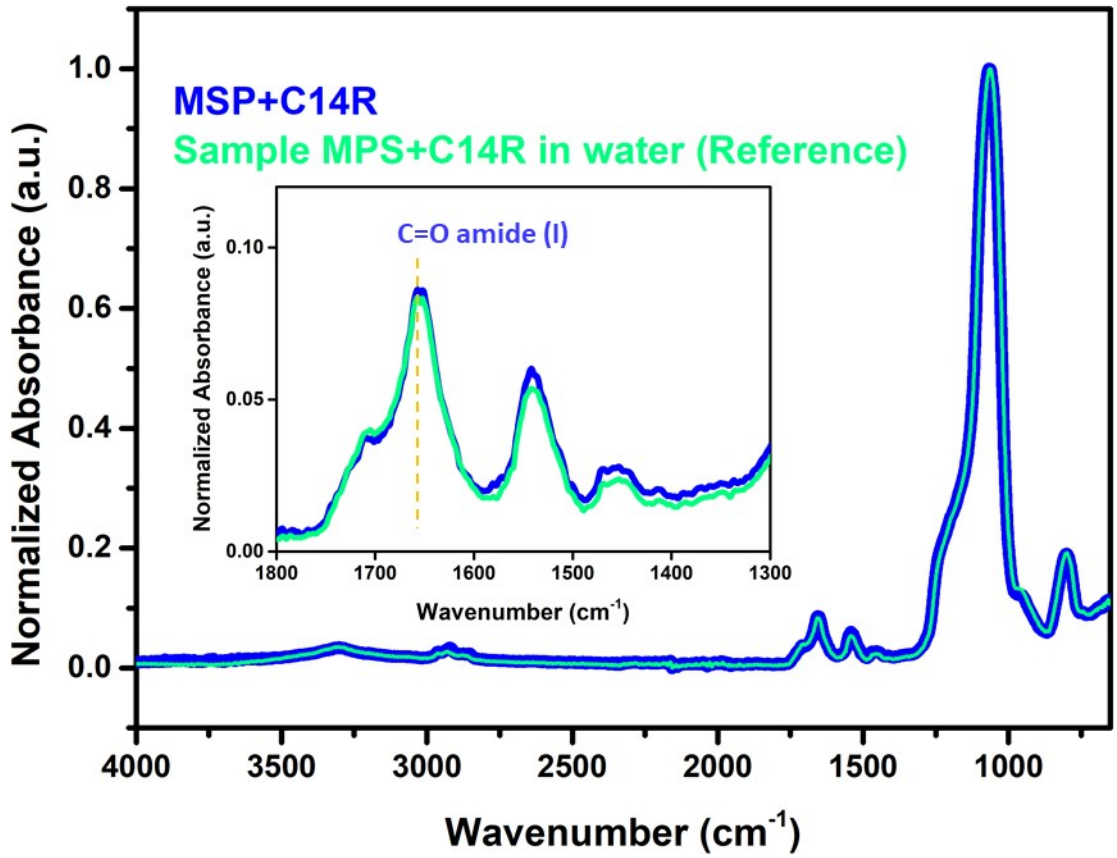

Figure S8. ATR-IR spectra comparing mesoporous silica particles functionalized with C14R (blue) to mesoporous silica particles functionalized with C14R subjected to a 40-minute immersion in water to indicates that the peptide stably remains inside the silica under the applied experimental condition, followed by drying (green).

Solvent Effects on C14R Peptide Release from Mesoporous Silica Particles

To investigate the effect of light scattering on peptide release from mesoporous silica particles, release was tested in the refractive index matching solvent DMSO. The ATR-IR spectra depicted the release of C14R peptide from mesoporous silica particles for a 2-hour period in PBS buffer (navy) and DMSO (green). The vibrational band at 1658 cm^{-1} associated with C=O (amide I) in the sample dissolved in DMSO exhibited a slightly stronger decrease compared to that in PBS. This observation suggests differences in the release behaviour attributed partially to the light scattering of the particle suspension (Figure S9, S10).

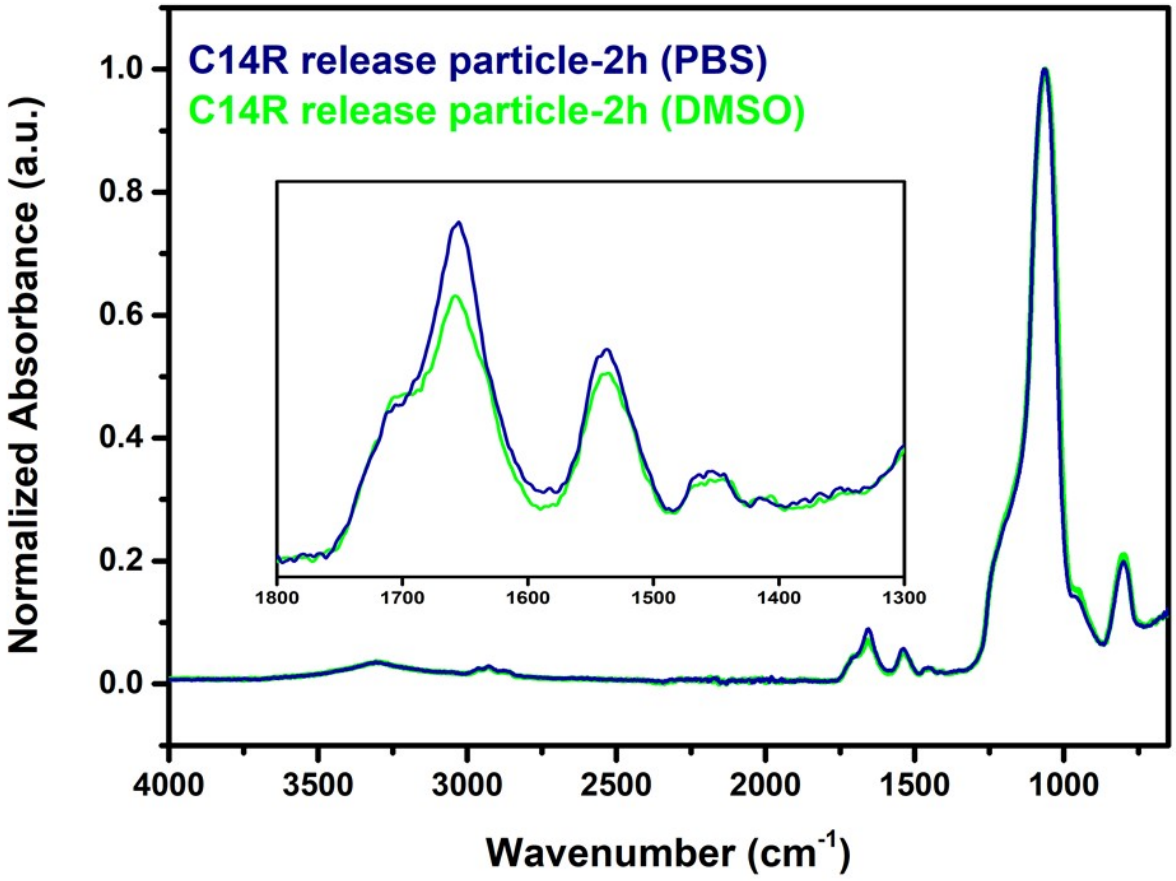

Figure S9. ATR-IR spectra illustrating the release of C14R peptide from mesoporous silica particles for 2h in PBS buffer (navy) and index matching DMSO (green).

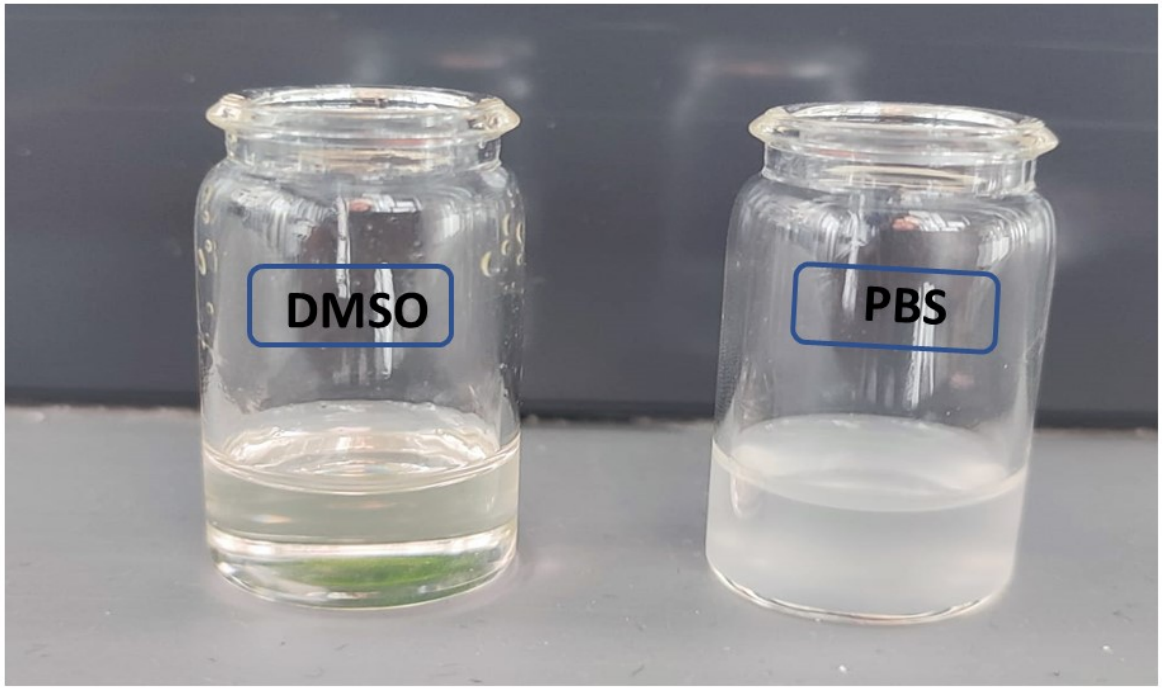

Figure S10. Right- mesoporous silica particles functionalized with C14R in PBS buffer. **Left**- mesoporous silica particles functionalized with C14R in DMSO.

Fluorescence Properties

The distance from the light source to the samples was modified to adjust the irradiation intensity for the light-triggered release. The power density of irradiation at the same area was measured using the optical power meter (NAME from THORLABS PM160T) at various distances. As the distance of 5 cm, the power density was determined to be 8.3 $mWcm^{-2}$. At a distance of 15 cm, the power density decreased to 1.2 $mWcm^{-2}$. At a power density of 8.3 $mWcm^{-2}$, the fluorescence intensity of the release solution was 30.3×10^4 a.u., while it decreased to 0.5×10^4 a.u. at 1.2 $mWcm^{-2}$ (Figure S11). As a result, a power density of 8.3 $mWcm^{-2}$ was maintained for the release experiments. To analyse the release solution containing the BODIPY labelled peptide, the fluorescence intensity in the solution was characterized. As the power density decreased with increasing the distance between the sample and the light source during irradiation for release, the fluorescent intensity in the solution decreased. The decreasing fluorescence indicates a decreased release of BODIPY-peptide in the sample solution (Figure S11). Additionally, bleaching did not seem to dominate the fluorescence changes, as the fluorescence increased in the solution after irradiation.

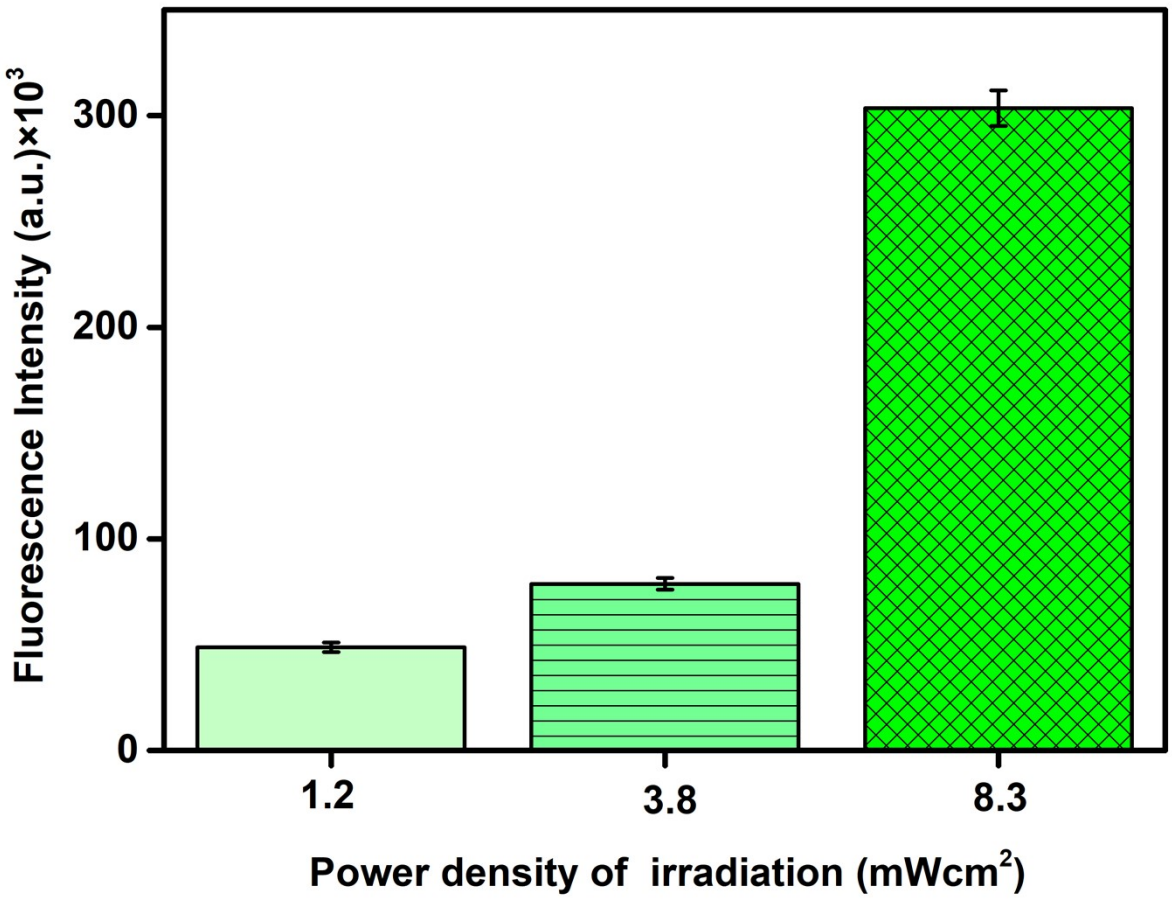

Figure S11. The fluorescence intensity of the release solution from film in dependence of the power density of the light source (Error bars represent the standard deviation of three films taken from one batch of functionalized mesoporous silica).

Impact of Irradiation Intensity on Time-dependent Peptide Release

The concentration of released peptide from particles demonstrates a clear dependence on irradiation intensity over time, as depicted in Figure S12. Increasing irradiation intensity is associated with increased peptide release (2, 4, 7, and 10 hours).

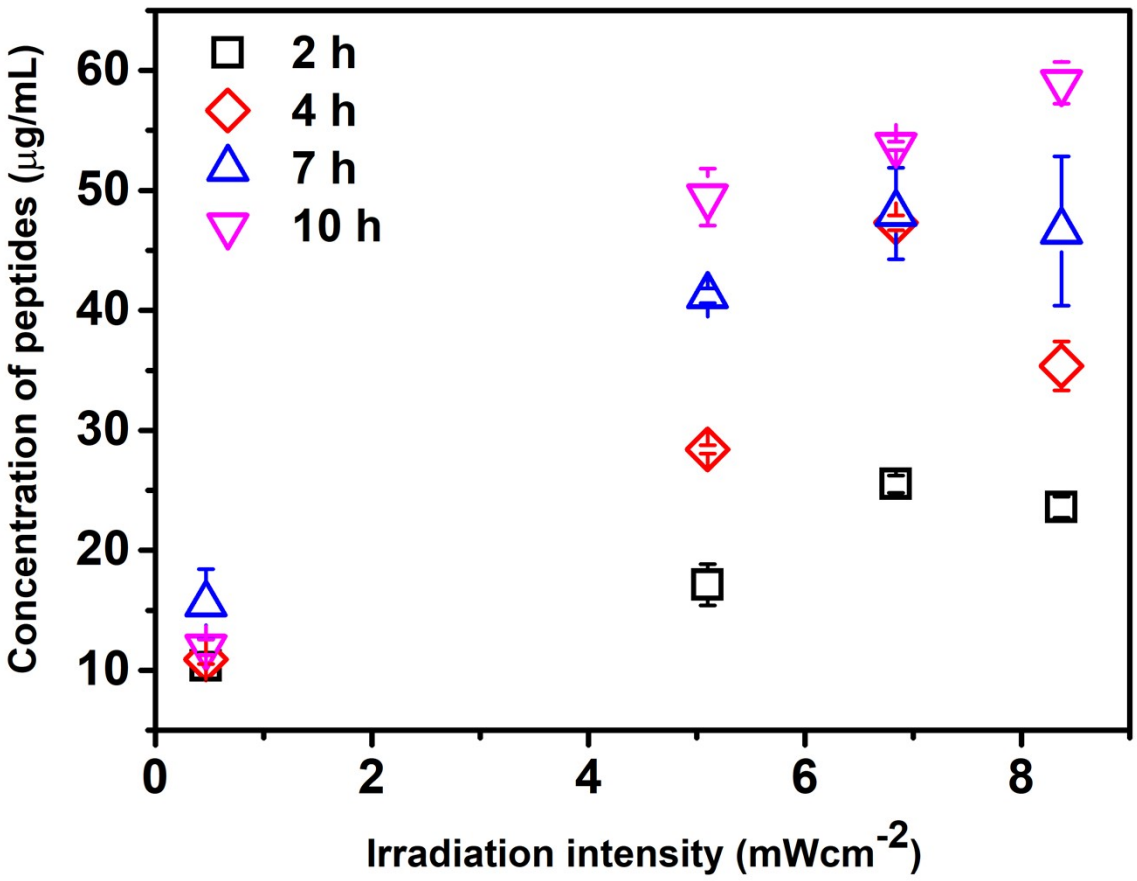

Figure S12. Released peptide concentration from C14R functionalized mesoporous silica particles under varying irradiation intensities over time (Error bars represent the standard deviation of three portions of particles from one batch of functionalized mesoporous silica particles). Results are presented for four time: 2 (□), 4 (◇), 7(△), and 10 (▽) hours (data from Figure 4g plotted in dependence of irradiation intensity)

Minimal Inhibitory Concentration (MIC) of C14R and Melittin Antimicrobial Peptide

To evaluate the efficacy of the antimicrobial peptide against *E. coli* BL21(DE3) with an empty pet26b (+) plasmid, a minimal inhibitory concentration (MIC) test was conducted. The observation indicated the optimal dosage of the antimicrobial peptide required for treating an infection (Table S3). To assess the antimicrobial effect of BODIPY linked peptide after release and dissolved peptide with the sequence RRRFRGDK, their influence on the growth of *E. coli* was investigated. The bacterial growth rate was evaluated by measuring the optical density at 600 nm at a concentration of 3 mg/ml antimicrobial peptide (Figure S12). The bacterial growth rate slightly decreased 12 h in the sample containing the BODIPY-peptide

antimicrobial agent as compared to the sample with the dissolved peptide of identical sequence RRRFRGDK but without BODIPY

Table S3. Minimal Inhibitory Concentration (MIC) of C14R and Melittin peptides on Gram-Negative Bacteria Strains.

Bacterial Strain	Antimicrobial Agent	Structure	MIC (mg/mL)	Method
E. Coli. **BL21(DE3) with empty pet26b (+) plasmid**	C14R peptide	CSSGSLWRLIRRFLRR	0.093	Broth Dilution
E. Coli. **BL21(DE3) with empty pet26b (+) plasmid**	Melittin	GIGAVLKVLTTGLPALISWIKR	0.093	Broth Dilution

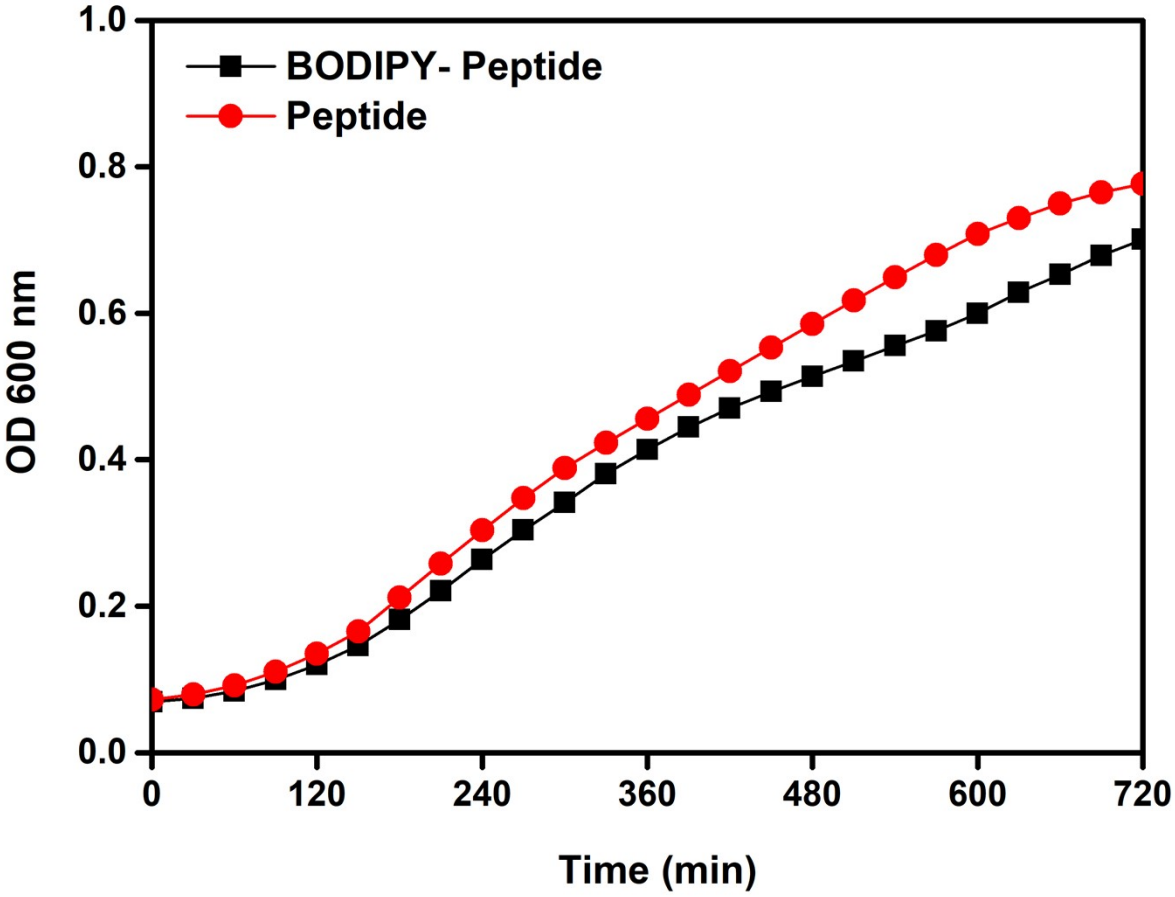

Figure S13. Growth curve of *Escherichia coli* cells cultured in kanamycin broth in the presence of a short model peptide RRRFRGDK (red), and in presence of BODIPY-short peptide RRRFRGDK (black).

CLSM Analysis: Impact of C14R Antimicrobial Peptide on *E. coli*

Confocal Laser Scanning Microscopy (CLSM) analysis was performed to explore the influence of the antimicrobial peptide on the membrane and permeability of *E. coli* (Figure S14). Imaging was conducted using a Leica SP8 CLSM, employing an HCX PL APO 63× NA 1.2 W CORR CS2 objective (BODIPY: ex. 488 nm, em. 505–525 nm; Nile Red: ex. 561 nm, em. 570–590 nm).

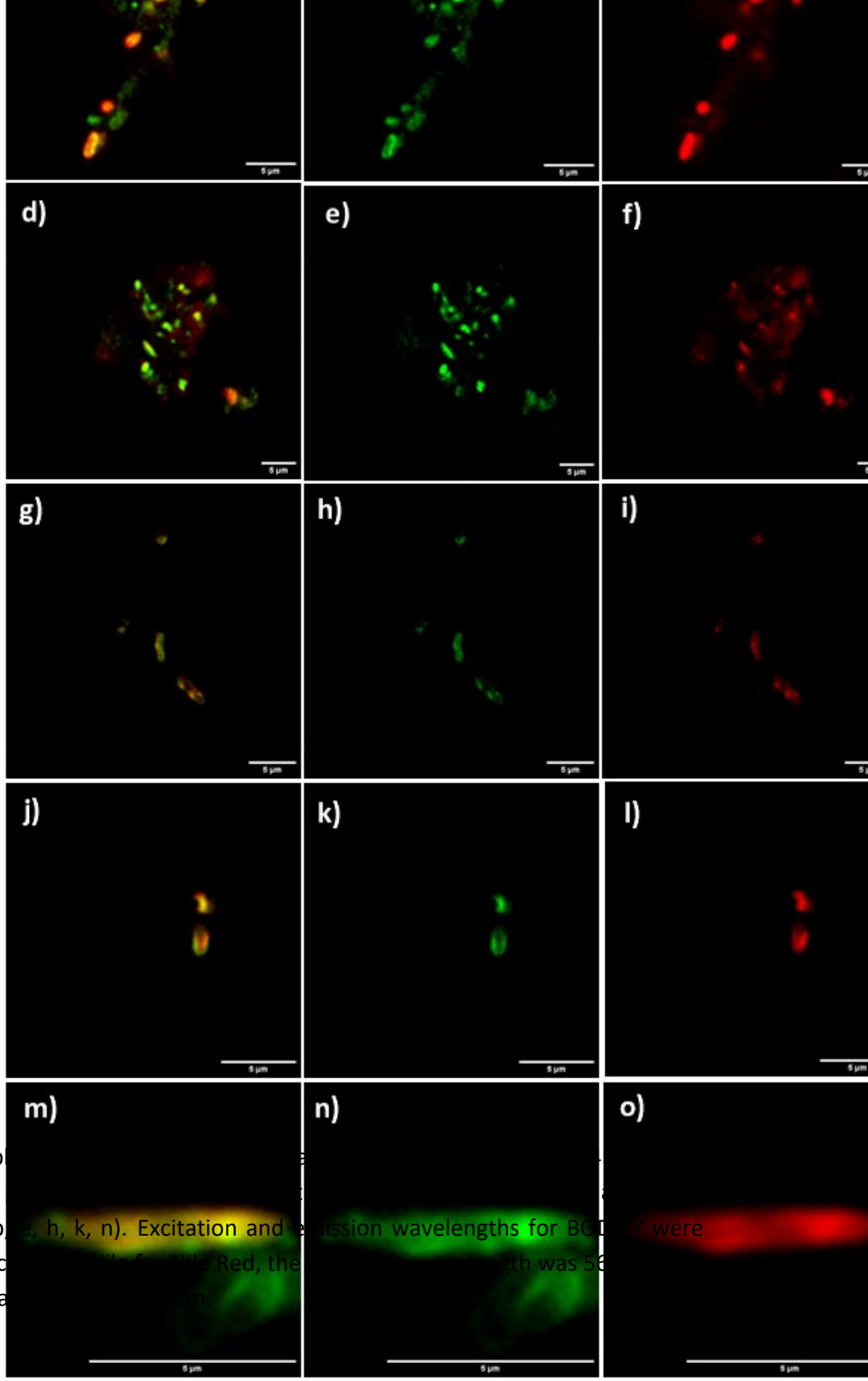

Figure S14. Confocal micrograph
BODIPY on an *E. coli* strain (a, d,
colour peptide C14R-labelled (b
488 nm and 505–525 nm, respec
emission were detected in the ra

AUTHOR INFORMATION

Corresponding Author:

Annette Andrieu-Brunsen, Department of Chemistry, Technical University of Darmstadt, Peter-Grünberg-Str. 8, 64287 Darmstadt, Germany. E–mail: annette.andrieu-brunsen@tu-darmstadt.de, Orcid.org/ 0000-0002-3850-3047

Author:

Mohadeseh Bagherabadi, Department of Chemistry, Technical University of Darmstadt, Peter-Grünberg-Str. 8, 64287 Darmstadt, Germany. Orcid.org/ 0000-0001-9031-5281

Author Contributions

‡All authors have given approval to the final version of the manuscript.

Notes

The authors declare no competing financial interest.